

Mixed-Mode Stress Intensity Factor Determination of Riveted Lap Joints Used in Aircraft Fuselage Structures

S. Suresh Kumar · H. Ashwin Clement · R. Karthik

Submitted: 16 February 2017 / Published online: 15 June 2017
© ASM International 2017

Abstract In the present work, mixed-mode stress intensity factor (SIF) of multiple cracks in a riveted lap joint has been determined, with and without the presence of stringer under two different (uniaxial and biaxial) loading conditions. Geometry correction factor (Y) has been determined with consideration of mode II and mode III fractures, and the effect of stringer on SIF of intermediate as well as edge cracks was investigated. Diametrically opposite surface cracks with various crack depth ratios (a/t) were considered for a typical longitudinal splice joint. At the crack middle region [$(S/S_0) = 0$], SIF of cracks estimated under uniaxial loading condition reduces gradually with crack depth ratio due to frictional contact, whereas in the case of biaxial loading, higher SIF was observed at lower crack depths [$(a/t) = 2$]. The presence of stringer reduces the SIF of multiple cracks as it decreases the secondary bending moment caused by the eccentric loading. Compression of crack surfaces is observed at regions closer to crack middle [$(S/S_0) = -0.33$] due to the presence of stringer, and mode I fracture was observed to be dominant at the crack surface region [$(S/S_0) = \pm 1$]. Influence of mode II fracture is higher at the crack middle region due to crack interaction in unstiffened plates, whereas the effect reduces with the presence of stringer. A three-parameter relationship has been developed to estimate the SIF of multiple cracks in a riveted lap joint. The residual life of the riveted joints can be determined from the calculated mixed-mode SIF.

Keywords Stress · Intensity factor · Mixed-mode fracture · Biaxial loading · Crack depth ratio · Stringer

List of symbols

a	Crack length (mm)
t	Thickness of the sheet (mm)
S_0	Points along the crack front
(a/t)	Crack depth ratio
Y	Geometric correction factor
S/S_0	Location ratio
σ_h	Hoop stress (MPa)
σ_e	Longitudinal tension (MPa)
P	Internal pressure (MPa)
R	Radius of the fuselage (mm)
σ	Far field loading (MPa)
K_I	Mode I stress intensity factor ($\text{MPa}\sqrt{\text{m}}$)
K_{II}	Mode II stress intensity factor ($\text{MPa}\sqrt{\text{m}}$)
K_{III}	Mode III stress intensity factor ($\text{MPa}\sqrt{\text{m}}$)
K_{mix}	Effective stress intensity factor ($\text{MPa}\sqrt{\text{m}}$)
f	Friction coefficient

Introduction

The primary role of an aircraft fuselage structure during its life is to carry loads and provide required lift force. This is achieved by using thin-walled structures whose interior surfaces are reinforced by longitudinal and transverse strengthening members called stiffeners. Riveted lap joints are being used traditionally for long time in the aerospace industry. These joints are considered as the crucial zones that are designed under damage tolerance procedures in the civil aircraft industry. Multi-site damage (MSD) is the

S. Suresh Kumar (✉) · H. Ashwin Clement · R. Karthik
Department of Mechanical Engineering, SSN College of Engineering, Kalavakkam, Chennai 603 110, India
e-mail: sureshkumars@ssn.edu.in

preeminent failure mode of a longitudinal splice joint due to the fatigue load induced by cabin pressurization cycle. MSD in aging aircraft is mainly due to clamping force deterioration which results from corrosion or fretting under cyclic loading and excessive out-of-plane deformations during service operations [1]. The significance of MSD in structural integrity of fuselage was realized immediately after the Aloha and Japan Airlines crash incidents. MSD is an important concern in aging aircraft and deals with determining failure conditions for multiple crack configurations. Compared to single-site damage (SSD), MSD reduces the life expectancy of a joint by 30%. Thus, determination of residual life of the joints is the primary concern during their design. Prediction of the life of the joint involves three phases: life until crack initiation, stable fatigue crack growth and unstable rapid MSD growth to failure. The structural integrity of the riveted joint with multiple cracks depends on the length of each crack, its orientation with respect to the other and the distance between cracks and the severity of stresses at the crack tips. These crack tip stresses are defined by stress intensity factor (SIF). The SIF solutions obtained could be useful for correlating fatigue crack growth rates. Also they can be used to compute fracture toughness of riveted joints which have surface cracks at the plate.

Literature Review

Many researchers [2–5] have made an attempt to determine the SIF of cracks in a riveted lap joints using numerical and experimental technique. Hertel [6] observed increased fatigue life properties with the presence of stiffeners due to increased stiffness around the rivet. Vlieger [7] noted that addition of stiffener in the middle row does not affect fatigue behavior unless stiffener rotation is constrained. Terada [1] estimated that the crack growth life for the panel without MSD was 2.5 times longer than for the panel with MSD. Szolwinski et al. [8] observed that when applied loading starts increasing, only the friction force transmits the load. Fracture analysis by Schijve [9] clearly suggested that fretting of sheets and rivet heads leads to multiple crack initiation. Schijve [10] experimentally observed that secondary bending moment is unfavorable as they cause increase in stress concentrations near the rivet holes. Muller's crack growth experiments [11] under different loading conditions showed that biaxial loading resulted in considerably faster crack growth due to the out-of-plane deformations. Soetikno [12] have analyzed the influence of rivet types and suggested that countersunk rivets have lesser static strength.

As suggested, the influence of stringers on overall fatigue life is insignificant, and moreover, difficulty in

arresting stringer rotation led many researchers to neglect the effect of stringer in their test specimens. However, maximum stress concentration occurs at the region where the stringer is connected to the sheets, as it restricts the out-of-plane deformations. Thus, in order to predict the fracture parameters, with greater accuracy, the effect of stringer has been considered in the current work and compared with the unstiffened panel. The literature studies clearly emphasize that fracture analysis involving single crack is no more conservative, and hence, multiple cracks were considered in the present work. Also to understand the effect of edge crack and crack interaction, both symmetric and edge cracks were introduced in the model. Since the type of rivets, loading conditions, size of the specimens and frictional force have considerable influence on the calculated values, care has taken in approximating them as close as possible to service condition. Presently, the analysis model is made up of countersunk rivets loaded both in uniaxial and biaxial conditions with frictional contact between the interfaces. The main objective of the present work is

1. To determine mixed-mode SIF of longitudinal splice joint with multiple cracks.
2. To understand the effect of stringer on SIF of multiple cracks for various crack depth (alt) ratios.
3. To investigate the effect of loading condition (uniaxial and biaxial) on SIF.
4. To develop a three-parameter relationship between crack depth ratio (alt), location ratio (S/S_0) and geometry correction factor (Y).

3D fracture analysis of longitudinal splice joint (B737-200) with multiple cracks has been investigated. The splice along the fuselage neutral line was chosen for analysis. This is mainly to include the hoop stresses on the joint. SIF has been determined at the crack tips for crack depth ratio (alt) ranging from 2 to 5. Through cracks of larger length (in depth direction) were considered for the present analysis because most of the crack growth prediction experiments done by linear elastic fracture mechanics (LEFM) approach on small cracks led to the conclusion that behavior of small cracks is anomalous, and thus, the results are not reliable. Two loading conditions have been considered, and a comparison was made between uniaxial loading (hoop tension only) and 'in-phase' biaxial loading (hoop and longitudinal tension).

Finite Element Model of the Riveted Lap Joint

The longitudinal splice joint was modeled and analyzed using finite element code ABAQUS. A 3D model of the joint (Fig. 1) with three rows of rivets was considered with

dimensions of each sheet being 90 mm × 70 mm. In the stiffened panel, a stringer of dimensions shown in Fig. 2 was modeled. A total of 100° flush rivets were modeled with a shank diameter of 4 mm, and a total of nine rivets were assembled to the sheets in a 3 × 3 matrix. The sheets to be riveted have totally nine holes each, and the outer sheet is provided with 100° countersunk recess to support the rivet. Three holes were also made in the stringer, so that they can be fixed to the plates. Countersunk recess is provided in the outer sheet up to 3/4th of its sheet thickness to avoid knife-edge effect. The rivets were then assembled in the respective holes in the sheets along with stringer. The assembled 3D model is shown in Fig. 2.

Material properties of different grade aluminum were considered for the sheets, stringer and rivets, and their properties are listed in Table 1. Through cracks of same crack length (a) were introduced on the either side of the rivet holes such that the crack plane is normal to the applied hoop tension. Four different models with differing crack depth ratios ($a/t = 2, 3, 4, 5$) were modeled separately and analyzed. Boundary conditions were chosen so that they simulate service conditions and were applied to facilitate mixed-mode fracture.

‘Surface-to-surface’ contact interaction was defined between (i) rivet hole to rivet region, (ii) rivet head to sheet

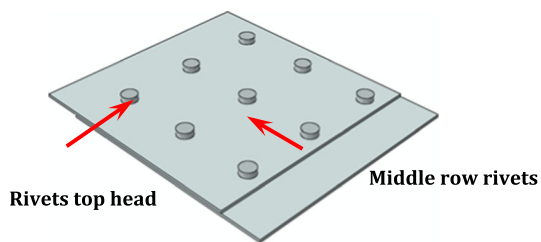


Fig. 1 3D model of stiffened pane without stringer

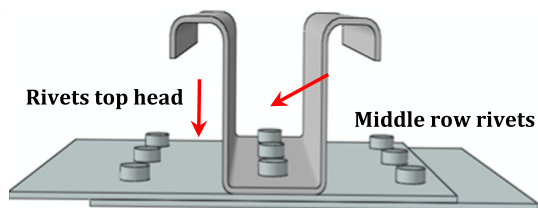


Fig. 2 3D model of stiffened panel with stringer

region, (iii) sheet to sheet region and (iv) stringer to sheet region. Frictional contact was defined between these interfaces with a friction coefficient ($f = 0.1$) as friction transmits major part of the load and leads to MSD. There was no interference or clearance between the rivet hole and the rivet region. Cracks were introduced on either side of each rivet (Fig. 3) at the middle row initiating from the rivet hole such that they will be presenting in all two or three layers. All cracks have the same crack length ($a = 1.8$ mm, 2.7 mm, 3.6 mm, 4.5 mm for ratios $a/t = 2, 3, 4, 5$, respectively). The region around the crack front was partitioned into five circular contours to provide fine mesh around the crack front and thus facilitates more accurate results. The cracks in the middle row are shown with the circular contours. Meshed 3D models are shown in Figs. 4 and 5. A total of 20-node quadratic brick elements was used to obtain higher accuracy of results. Fine mesh was considered near the middle row and the contact interaction regions for facilitating better convergence.

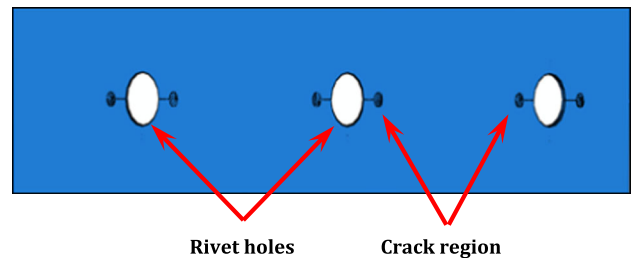


Fig. 3 Cracks in the middle row of FE model

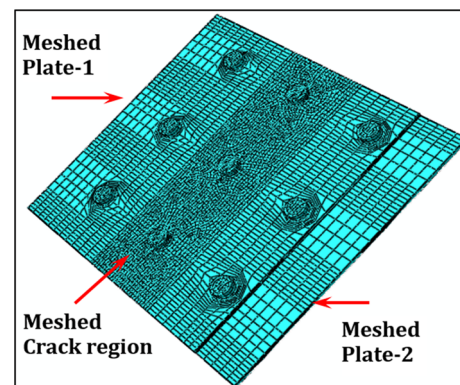


Fig. 4 Meshed FE model of stiffened panel

Table 1 Material properties of riveted lap joint

Part	Material	Young's modulus (GPa)	Poisson's ratio	Yield stress (MPa)
Sheets	Aluminum (2024-T3 Alclad)	73.0	0.33	276
Rivet	Aluminum (2117 T4)	71.0	0.33	165
Stringer	Aluminum (7075-T6 Clad)	71.7	0.33	482

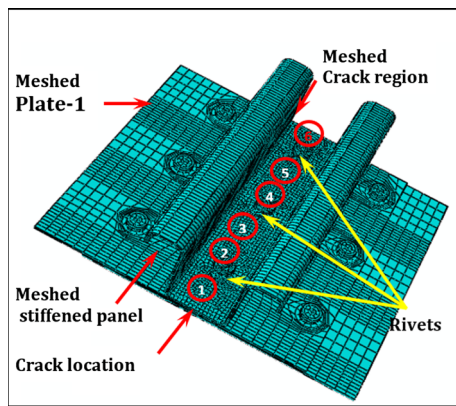


Fig. 5 Meshed FE model of stiffened panel with stringer

Contour Integral Evaluation

In the present work, ‘contour integral evaluation’ approach has been used to estimate the SIF values around the crack region. To simulate the theoretical inverse square root singularity of stresses and strains, near the crack border singular elements were arranged. If all the midface nodes of the 20-node quadratic brick elements are moved to their quarter points closest to the crack line, the variations in the local stress and strain fields can be minimized. Due to 3D nature of the crack advancement, crack propagation direction cannot be predicted, and hence, ‘crack plane normal’ criteria were used to define the crack propagation direction.

Determination of Mixed-Mode SIF

When the riveted joint is mechanically loaded, the cracks may simultaneously open and slide relative to each other. The mixed-mode fracture is formed in a joint due to complex loading condition or crack location. In the present work, mixed-mode SIF is calculated for opposite cracks located in a riveted joint using FEM approach. Far field tensile load was applied to the joint which causes the cracks to open and SIF values were calculated along the crack border. Currently the geometry correction factor (Y) was calculated from mixed-mode fracture which includes the additional effect of mode II and mode III fractures. The mixed-mode SIF was calculated from the following relation.

$$K_{mix}^2 = K_I^2 + K_{II}^2 + (K_{III}^2)/(1 - \nu) \tag{Eq 1}$$

$$K_{mix} = Y\sigma\sqrt{\pi a} \tag{Eq 2}$$

$$Y = K_{mix}/(\sigma\sqrt{\pi a}) \tag{Eq 3}$$

where Y is the geometry correction factor, a crack length (mm), σ far field stress (MPa).

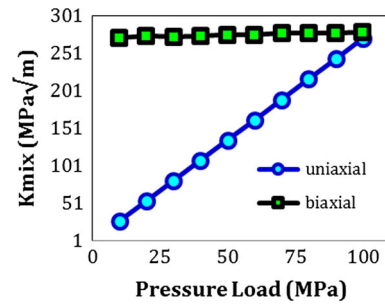


Fig. 6 Behaviour of K_{mix} for varying (σ_h) in uniaxial specimen and varying (σ_l) with constant ($\sigma_h = 100$ MPa) in biaxial specimen

Table 2 Test matrix for numerical simulation

Structure name	Loading conditions	
	Uniaxial loading	Biaxial loading
Unstiffened panel	$alt = 2$	$alt = 2$
	$alt = 3$	$alt = 3$
	$alt = 4$	$alt = 4$
	$alt = 5$	$alt = 5$
Stiffened panel	$alt = 2$	$alt = 2$
	$alt = 3$	$alt = 3$
	$alt = 4$	$alt = 4$
	$alt = 5$	$alt = 5$

While computing the geometric correction factor for the uniaxial loading, the hoop stress (σ_h) was considered as the far field stress (σ). In case of biaxial loaded joints, since the load varies on both the X-axis and Y-axis, the far field stress (σ) cannot be considered directly as hoop stress (σ_h). Thus, an attempt has been made numerically on a center cracked plate, to understand the load behavior (uniaxial and biaxial) during SIF determination. The variation is plotted in Fig. 6. Initially, the hoop stress (σ_h) was increased gradually for a uniaxially loaded condition and the corresponding SIF was calculated. In the case of biaxial loading, the hoop stress ($\sigma_h = 100$ MPa) was kept constant, and simultaneously the longitudinal stress (σ_l) was varied in gradual increments. It is noted that the K_{mix} value remains constant irrespective of the variation in longitudinal stress which is parallel to the crack surface. This is due to the fact that mode I fracture significantly dominates compared to other modes of fracture, and thus, a far field load of 100 MPa was considered.

The fatigue crack growth rate and residual life of the joint can be calculated from Paris equation, and Table 2 shows the test matrix of loading conditions considered in the present work.

Load Calculation

In uniaxial loading, only the hoop tension was considered. For unstiffened panel, the hoop stress can be calculated using the analytical expression given as

$$(\sigma_h) = PR/t \quad (\text{Eq 4})$$

Using $R = 3.23$ m, $t = 1.6$ mm and altitude of 45,000 sqft yields 120 MPa. According to Niu [13], it must vary between 80 and 120 MPa. Thus, $\sigma_h = 100$ MPa has been considered. In biaxial loading, both hoop tension and longitudinal tension were considered. For unstiffened panel, the biaxiality ratio was 0.5, and thus, longitudinal stress $\sigma_1 = 0.5 (\sigma_h) = 50$ MPa was selected. For stiffened panel, the biaxiality ratio was slightly less than 0.5. But for the purpose of comparison, the loads considered for stiffened panel are same as those of unstiffened panel. Figure 6 shows the SIF variation for uniaxial and biaxial loading conditions. Normalized coordinate system was used to define the points along the crack front. $S/S_0 = 0$ indicates the middle region of the crack front, whereas $S/S_0 = \pm 1$ indicates the top and bottom side of the crack surface, respectively.

Result and Discussion

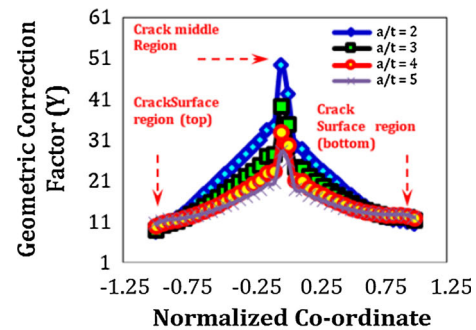
SIF of multiple cracks in a riveted lap joint with and without the presence of stiffened panel was calculated numerically under two different loading conditions (uniaxial and biaxial). The influence of crack depth ratio, loading condition and stringer on mixed-mode SIF of riveted lap joint has been investigated.

Effect of Crack Depth Ratio (a/t) on SIF of Unstiffened Riveted Lap Joint

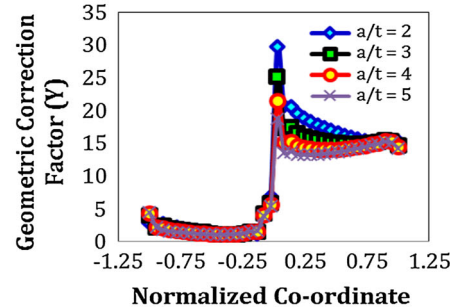
Figure 7 shows the effect of crack depth ratio on SIF of multiple cracks in an unstiffened panel subjected to uniaxial loading. As the crack depth ratio increases, SIF decreases considerably at the crack middle region [$(S/S_0) = 0$]. Cracks 1 and 3 show a similar trend, whereas crack 2 which is located at the middle of cracks 1 and 3 shows a sudden increase in SIF values due to interaction effect of cracks 2 and 3. Since the middle region corresponds to the interface between plates, a crossover in SIF trend was observed.

Effect of Crack Depth Ratio (a/t) on SIF of Stiffened Panel Under uniaxial Loading

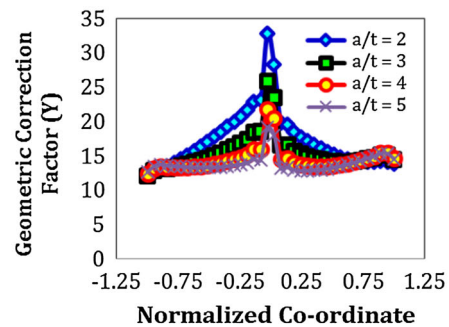
Figure 8 shows the SIF variation of multiple cracks in stiffened panel subjected to far field uniaxial loading



(a) Crack 1



(b) Crack 2



(c) Crack 3

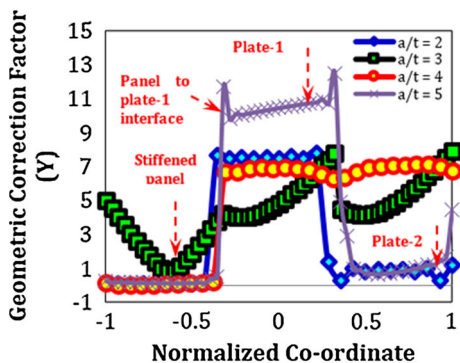
Fig. 7 Effect of crack depth ratio on SIF of unstiffened panel—uniaxial loading.

condition. Compared to unstiffened model, SIF values of stiffened panel are lower (Fig. 8). The presence of the stringer reduces the secondary bending moment caused by the eccentric loading, and lower SIF values are observed at the region of [$(S/S_0) = 0$ to $(S/S_0) = -0.33$]. A sudden crossover in SIF is observed at [$(S/S_0) = -0.33$] which is due to the gap between panel and plate 1. In between the range of [$(S/S_0) = -0.33$ to $(S/S_0) = 0.33$], constant SIF is observed at lower crack depths for uniaxial loading conditions. As the crack depth ratio increases, SIF also increases considerably. Sudden reduction in SIF trend is mainly due to friction between plates 1 and 2. In contrast to unstiffened model, SIF values increase with crack depth ratio (a/t) with stiffened plate model. Since the effect of panel is limited up to plate 1, non-uniform SIF variation is observed between crack 1 and crack 3. Since the bottom

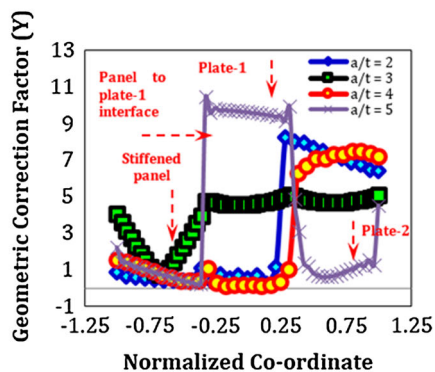
plate is independent of stringer effect, increasing trend of SIF is observed at lower crack depths due to higher secondary bending moment caused by eccentric loading.

Effect of Crack Depth Ratio (a/t) on SIF of Unstiffened Panel Under Biaxial Loading

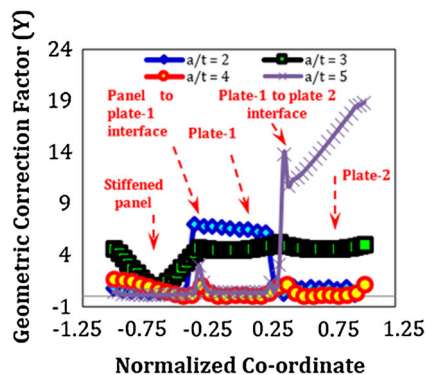
SIF of riveted lap joint subjected to biaxial loading is shown in Fig. 9. In contrast to uniaxial loading, SIF of multiple cracks is higher, only at lower crack depths [$(a/t) = 2$], whereas at higher crack depths, SIF values are



(a) Crack-1

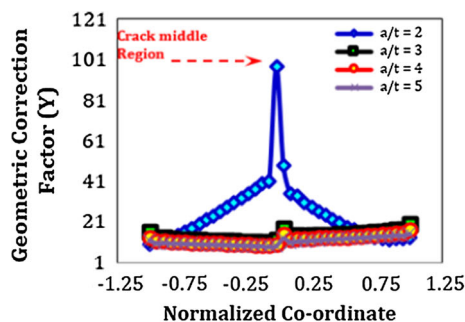


(b) crack-2

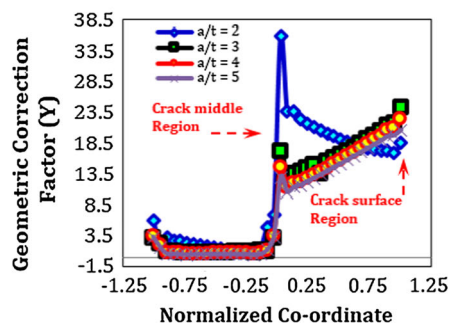


(c) Crack3

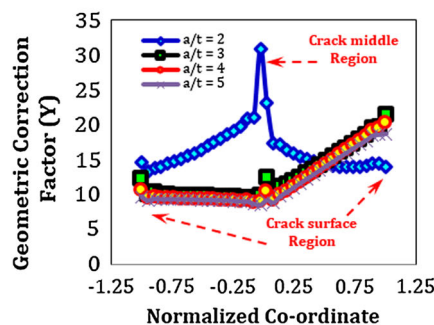
Fig. 8 Effect of crack depth ratio on SIF of stiffened panel—uniaxial loading.



(a) Crack-1



(b) crack-2



(c) Crack3

Fig. 9 Effect of crack depth ratio on SIF of stiffened panel—biaxial loading.

Table 3 Parametric relationship for geometry correction factor

Crack no.	Relation
Crack 1, crack 2 and crack 3	$Y = P00 + p10 \times x + p01 \times y + p20 \times x^2 + p11 \times x \times y + p02 \times y^2 + p30 \times x^3 + p21 \times x^2 \times y + p12 \times x \times y^2$

Table 4 Coefficients of polyfit equation

Coefficients	Crack 1	Crack 2	Crack 3
P00	64.12	37.96	41.09
P10	-12.02	-4.573	-9.117
P01	-0.07372	8.77	-1.466
P20	1.439	0.1594	1.501
P11	0.729	-1.687	1.408
P02	-48.86	-27.6	-21.55
P30	-0.1116	-0.005657	-0.1233
P21	-0.1123	0.1828	-0.1846
P12	6.885	3.75	3.541
R ²	99.78	99.91	99.67

higher at the crack surface region (Fig. 9). At lower crack depths [(alt) = 2], negligible influence of loading condition was noted. Thus, one can expect higher crack growth rate at the crack middle region compared to crack surface region. Higher out-of-plane deformation of the plates is noticed for the biaxial loading condition compared to uniaxial loading.

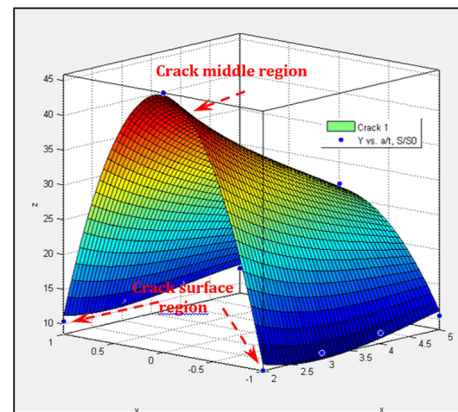
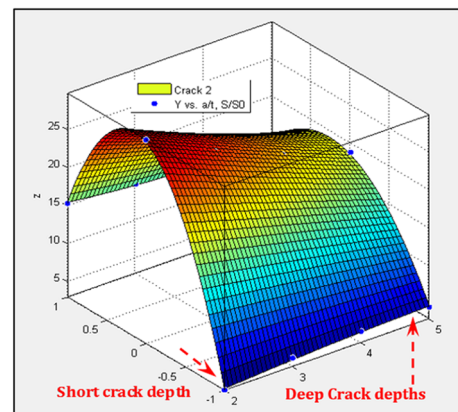
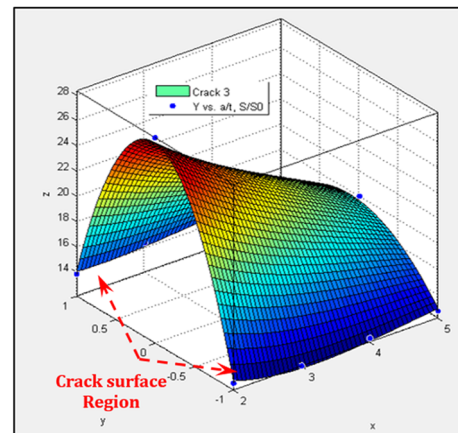
The effect of biaxial loading on SIF of multiple cracks in a stiffened panel was also calculated. Compared to uniaxial loading, SIF values were observed to be lower at the middle region of the crack. A reverse trend of SIF distribution was observed at the middle region of crack which is located at the plate 1.

The relationship between crack depth ratio (alt), crack location (S/S_0) and geometry correction factor (Y) is plotted in a 3D surface plot as shown in Fig. 10. X-axis indicates crack depth ratio, Y-axis indicates crack location (S/S_0), and Z-axis indicates geometry correction factor (Y). A three-parameter relationship (Table 3) was obtained to determine the SIF of riveted lap joints subjected to uniaxial loading conditions, and Table 4 provides the coefficient of polyfit equation. Using the relationship, one can determine the SIF and residual life of the joints from crack growth rate data using the Paris equation.

Table 3 provides the three-parameter relationship for the estimation of geometry correction factor of riveted lap joint subjected to uniaxial loading condition. The residual life of the joint can be estimated using Paris fatigue crack growth equation

$$(da/dN) = C\Delta K^m \quad (\text{Eq 5})$$

where C and m are material constants. Since the influence of mode II and mode III fractures has also been considered in the present work, one can use the relationship to determine the residual life of the stiffened and unstiffened panel. The coefficients of polyfit equations are given in Table 4.

**(a)** Surface plot for crack-1**(b)** Surface plot for crack-2**(c)** Surface plot for crack-3**Fig. 10** Surface plots of geometry correction factor (Y) for various cracks

Conclusions

SIF of multiple cracks in riveted lap joint subjected to far field uniaxial and biaxial loading condition has been investigated numerically for various crack depth ratios. The following conclusions are obtained from the analysis.

As the crack depth ratio (a/t) increases, SIF estimated under uniaxial loading decreases gradually at the crack middle region [$(S/S_0) = 0$] due to frictional resistance. In the case of biaxial loading, SIF values are higher at lower crack depths [$(a/t) \leq 2$]. Gradual increase in SIF is observed from the middle region [$(S/S_0) = 0$] toward bottom of the plate [$(S/S_0) = +1$] in comparison with uniaxial loading.

It is noted that the presence of stiffened panel reduces the SIF of multiple cracks to a greater extent as it reduces the secondary bending moment caused by the eccentric loading. In contrast to unstiffened model, SIF increases with crack depth ratio at the middle region [$(S/S_0) = 0$] of the crack front both for the uniaxial and biaxial loading conditions.

Both positive mode I fracture and negative mode I fracture are observed for the middle crack (crack 2) irrespective of the loading conditions considered. Compression of crack surface was observed at regions closer to [$(S/S_0) = \pm 0.33$] for a plate with stiffened panel.

The presence of stiffened panel affects the load pattern of the plate and causes higher influence of mode II fracture at regions closer to the crack middle. A three-parameter relationship has been developed to determine the SIF of multiple cracks in a riveted lap joint for residual life prediction.

Acknowledgments This work was financially supported by the management of SSN College of Engineering, Chennai, India.

References

- H. Terada, A proposal on damage tolerant testing for structural integrity of aging aircraft-learning from JAL accident in 1985. *Fract. Mech.* **25**, STP 1220 (1995)
- M. Skorupa, T. Machniewicz, A. Korbel, Fatigue crack location and fatigue life for riveted lap joints in aircraft fuselage. *Int. J. Fatigue* **58**, 209–217 (2014)
- M. Skorupa, A. Skorupa, T. Machniewicz, A. Korbel, Effect of production variables on the fatigue behaviour of riveted lap joints. *Int. J. Fatigue* **32**(7), 996–1003 (2010)
- In Erdogan, F. (ed.) *Fracture Mechanics. ASTM STP 1220*, 25 (ASTM, Philadelphia, 1995), pp. 557–574
- L.F.M. da Silva, J.P.M. Goncalves, F.M.F. Oliveira, P.M.S.T. de Castro, Multiple-site damage in riveted lap-joints: experimental simulation and finite element prediction. *Int. J. Fatigue* **22**(4), 319–338 (2000)
- H. Hertel, *Fatigue Strength of Structures* (Springer-Verlag, Berlin, 1969)
- H. Vlieger, Results of uniaxial and biaxial tests on riveted fuselage lap joint specimens, in *Proceedings of FAA/NASA International Symposium of Advanced Structural Integrity Methods for Airframe Durability and Damage Tolerance*, Hampton, VA, 4–6 May 1994. NASA CP 3274, pp. 911–930
- M.P. Szolwinski, G. Harish, P.A. McVeigh, T.N. Farris, The role of fretting crack nucleation in the onset of widespread fatigue damage: analysis and experiments, in *Proceedings of the FAA–NASA Symposium on the Continued Airworthiness of Aircraft Structures*, Atlanta, Georgia, 1997, ed. by C.A. Bigelow, W.J. Hughes, pp. 585–596
- J. Schijve, Multiple site damage of riveted joints, in *International Workshop on Structural Integrity of Ageing Airplanes, Durability of Metal Aircraft Structures* (Atlanta, 1992), pp. 2–27
- J. Schijve, Multiple-site damage in aircraft fuselage structures. *Fatigue Fract. Eng. Mater.* **18**, 329–344 (1995)
- R.P.G. Muller, *An Experimental and Analytical Investigation on the Fatigue Behavior of Fuselage Riveted Lap Joints. The Significance of the Rivet Squeeze Force and a Comparison of 2024-T3 and Glare 3*, Ph.D. thesis (Tu Delft, Delft, 1995)
- T.P. Soetikno, *Residual Strength of the Fatigued 3 Row Riveted Glare3 Longitudinal Joint*, Master Thesis (Aerospace Engineering, Delft University of Technology, 1992)
- M.C.Y. Niu, *Airframe Structural Design: Practical Design Information and Data on Aircraft Structures*, 2nd edn. (Hong Kong Conmilit Press limited, 1999)